

Near Infrared Sintering of a cost effective Roll to Roll water purification coating

I. Mabbett*, D. Brennan*, N.P. Lavery**, C.M.E. Charbonneau***, K. Khan***, R. Woods***, A.B. Pursglove***, D.T. Bryant****, T.M. Watson*** and D.A. Worsley***

*Materials and Manufacturing Academy, Swansea University, Baglan Bay Innovation and Knowledge Centre, SA12 7AX, UK, i.mabbett@swansea.ac.uk

** College of Engineering, Swansea University, SA2 8PP, UK

***SPECIFIC, Swansea University, Baglan Bay Innovation and Knowledge Centre, SA12 7AX, UK

**** Imperial College London, SW7 2AZ, UK

ABSTRACT

Near Infrared (NIR) at 250kW/m² has been shown to sinter titanium dioxide (TiO₂) on metal based substrates in just 12.5s. This coupled with a screen printable hybrid titania paste with nano-particulate anatase attached to a mesoporous framework enables roll to roll manufacture of a highly photoactive water purification coating. Photocatalytic breakdown of organic molecules has been exemplified by the complete photobleaching in 1/3 sun UV irradiation of 10ppm indigo carmine dye solutions used to simulate textile dying industry effluent in developing nations. Moreover this has been achieved in 5-10 minutes using the enhanced surface area of modified nano-structured screen printed titania, as opposed to >12 hours using traditional titania pastes. The 12.5s NIR sintering step replaces a 30min 500°C convective heating step and as such reduces the bottleneck on line speed of oven length vs dwell time, enabling rapid roll to roll production. Computational Fluid Dynamics and Finite Element Analysis have been used to model the heat equation within the system with Monte-Carlo ray tracing being used to calculate the radiative flux distribution and view factors within various oven configurations. Complications such as wavelength shift on dimming and conductive heat flows have been calculated or treated empirically and fed into models.

Keywords: NIR, sintering, modelling, titanium dioxide, water purification

1 INTRODUCTION

Water scarcity is a growing problem across the world as population grows and with it so does water demand. Large areas of the globe are now at risk of physical or economic scarcity. A comprehensive study of conventional pollutants around the world and associated conventional purification techniques [1] are beyond scope of this work. However, it is noteworthy that dyed effluents from textile mills can cause significant problems via competition for incident photons between chromophores of the dye and plankton forming the basis of food chain so that photobleaching of effluent could improve biodiversity in many rivers in developing nations.

Infrared (IR) emitters are characterised by the type of IR radiation they emit, their operating temperature and by their

peak wavelength of emission [2]. Typical NIR emitters utilise tungsten-halogen filaments, operate at colour temperatures of between 2000-3140K and emit a broad spectrum of electromagnetic radiation, predominantly focused within the high energy density, near-wave IR subdivision of between 750-1400nm, with a peak wavelength of emission, λ_{max} , of around 900nm at maximum operating temperature. Heating is achieved by irradiating the coating with this broad spectrum of electromagnetic energy. NIR curing technology is becoming popular within coil coating industries for producing prepainted galvanised steel strip for the construction sector [3] at elevated line speeds of 150–180mmin⁻¹.

In Swansea there is expertise on NIR heating of metal substrates developed through work on curing of organic coated steels and [4] this work has been expanded to development of sintering steps addressing the bottlenecks in manufacture of metal based dye sensitized solar cells [5], silver and copper and conducting polymer inks[6,7,8] in printed electronics, flow melt tinplate [9] and galvanized steel through selective heating, speed up processing of battery materials [10] and heating of layers of active materials printed on glass [11].

NIR is becoming a popular option for rapid cure of coatings in the coil coating industry particularly where fast line speeds are required. The technology has the potential to reduce the cure time of a 20 μ m polyester coating on a galvanised steel substrate from around 30s via conventional heating methods down to <10s under the lamps [12]. Previous work suggested that the ideal situation in this case is to have a topcoat which is slightly transparent to NIR and an absorbing substrate to heat the coating from the substrate outwards in a two stage process which separates solvent removal from cross linking and film formation. TiO₂ is a white pigment used in many coatings and other products for its excellent reflectance and scattering properties, offering good hiding power. However, its photoactivity, left unmanaged, results in photodegradation due to photocatalytic breakdown of organic resins in a paint system for example [13]. These reflectance properties hold true in the visible region but in the NIR region the pigment becomes more transparent allowing radiation to penetrate to the substrate [14]. Galvanized steel has an absorption band in this region so can act as a hotplate and this is the basis for the empirical ideal suggested above.

The photoactivity of TiO₂ led to its use as a semiconductor for photovoltaics such as the dye sensitized solar cell [15] and more recently perovskite solar cells [16]. A limiting step to roll-to-roll production of dye-sensitized solar cells on metals is TiO₂ sintering (10–30 min). Building on learning from application to curing paint, NIR has been used to heat treat metal based dye-sensitized solar cells resulting a vastly reduced oven dwell time (12.5s) with no significant difference in cell efficiency [17]. NIR has also been shown to be useful in processing perovskite solar cells [18].

The working electrode of a metal based dye-sensitized solar cell is a metal substrate with a porous layer of TiO₂ sintered onto it, providing a high surface area photoactive semiconductor. To create the rest of the cell the layer would be dyed with a ruthenium dye and a transparent counter electrode would be introduced prior to sealing and filling with an iodide/triiodide electrolyte. However, if the manufacture is stopped after deposition and sintering of the TiO₂ then what is left is a high surface area UV active photocatalyst for the break down of organic material. This can be used to break down dye effluent from water or denature bacteria and since the catalysis is heterogeneous the process can be run continuously provided 1/3 sun UV is available at the photoactive surface, provided either naturally or artificially.

In order to optimize NIR heat treatment for the range of applications at Swansea, including water treatment, a transient finite difference thermal model has been formulated. The model is valid for spectrally selective surface coatings on any substrate material within an NIR furnace and is based on the heat equations. The irradiation from the NIR emitters provides the heat source and the model accounts for both radiative and convective cooling. A novel Monte Carlo ray tracing algorithm has been developed and is capable of determining the radiation view factor across a surface as well as for each node. The radiative flux is split into absorbed and reflected bands using UV-Vis-NIR reflectance spectra measured within the 250-2500nm wavelength range, enabling the model to predict the thermal build-up of coatings with very different absorption properties [19]. This applied across a range of coating, substrate and furnace combinations is an extremely useful tool in scaling up technology from laboratory bench to pilot line scale at SPECIFIC and beyond.

2 EXPERIMENTAL

2.1 Coating Deposition

Prior to TiO₂ deposition a thermocouple was spot welded directly onto the underside of the metal coupon to record an individual temperature profile. To enable deposition of the TiO₂ paste, a 1cm² mask of two layers of ≈50μm Scotch™ adhesive tape height guide was applied to the surface of the 1 mm thick metal (15 x 25 mm² titanium, stainless steel and galvanised steel). A paste containing

TiO₂ nanoparticles was placed onto the sample using a dropping pipette. Using a glass rod, this was drawn across the 1 cm² exposed titanium surface. Immediately following deposition of the TiO₂ the tape was removed leaving the TiO₂ layer on the metal substrate ready for thermal processing via conventional or NIR ovens.

Photocatalysts prepared in this way and sintered gave a TiO₂ film thickness of 6.5 (±1)μm determined using stylus profilometry.

2.2 NIR Sintering

NIR radiation falls between visible and infrared regions in the electromagnetic spectrum. For the purpose of this work we will refer to the NIR region as being between 800 and 1500nm, since the lamps used have an output in the range 250–2500nm peaking between 800 and 1000nm [20]. These wavelengths result in rapid thermal heating of metal substrates.

The NIR equipment used (AdPhos NIR/IR Coil lab V2) irradiates samples by moving a sample platform at a set speed (as determined by the operator) under the NIR lamp (set at a pre-set but variable power level) exiting the other side. Altering both the line speed and the NIR lamp power output enables a range of temperature profiles to be constructed. The samples were exposed at a range of power outputs for 12.5 s giving a range of peak metal temperatures (PMT) of between 545 and 880°C.

2.3 UV/Vis/NIR data

UV/Vis/NIR total reflectance spectra were recorded between 250 and 2500 nm for samples to input data into the computational model. Tests were carried out using a Perkin Elmer Lambda 750S high performance spectrophotometer.

UV/Vis spectrophotometry was also used to quantify the degree of dye breakdown. These readings are taken using a single beam Perkin Elmer Lambda XLS to determine the absorbance measurement of a dye solution taken via a flow cell during irradiation with three UV lamps (366nm) assembled in a rig giving approximately 0.3 suns of UV irradiation. The bottom of this rig was placed 50mm above the substrate.

2.4 Modelling

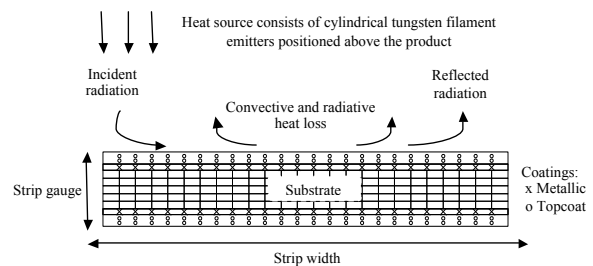


Figure 1: Geometry of the problem, showing the modelled heat transfer mechanisms

A model has been produced to predict the heating profiles of combinations of substrates and coatings in NIR furnaces and that model is described here. [19] Fig.1 shows the heat transfer mechanisms accounted for by the model. Radiative heat transfer occurs between the NIR emitters and the product surface, and radiative and convective heat transfer occurs between the environment and the product surface. The model assumes that the tungsten-halogen NIR lamps are diffuse, grey emitters, all surfaces are opaque and that the medium within the furnace is non-participating.

$$q_{irrad} = \epsilon_e \sigma F_{ij} A (T_c^4 - T_s^4) \quad (1)$$

The irradiative flux from the emitters, q_{irrad} , is determined by using Eqn.1, the Stefan-Boltzmann equation, where ϵ_e is the emissivity of the emitters, σ is the Stefan-Boltzmann constant, F_{ij} is the radiation view factor between the emitters and the product surface, A is the products surface area and T_c and T_s are the temperatures of the emitters and product surface respectively. The radiation view factor is calculated using a Monte Carlo ray tracing algorithm that is capable of yielding the average view factor across the surface and the infinitesimal view factor at each node. The incident flux is separated into absorbed and reflected bands through the calculation of the total absorptance coefficient, α , from UV-Vis-IR total reflectance spectra, within the 250-2500nm wavelength bands. The absorptance coefficient is obtained numerically by solving Eqn.2, where $E_{\lambda b}(\lambda, T_c)$, is Planck's law for the emissive power of a blackbody and $\alpha_\lambda(\lambda)$, is the spectral absorptance obtained from the spectral reflectance, $\rho_\lambda(\lambda)$, through the expression: $\alpha_\lambda(\lambda) = 1 - \rho_\lambda(\lambda)$, as the surface is opaque. Radiative heat losses are also described using the Stefan-Boltzmann equation. The model can account for natural and forced convective heat losses by calculating the convective coefficient, h , of the system empirically, in a process described in detail in [21].

$$\alpha = \frac{\int_0^\infty \alpha_\lambda(\lambda) E_{\lambda b}(\lambda, T_c) d\lambda}{\int_0^\infty E_{\lambda b}(\lambda, T_c) d\lambda} \quad (2)$$

The two-dimensional time-dependent conduction heat transfer equation with radiative flux and convective boundary conditions can be written as:

$$\rho C_p \frac{\partial T}{\partial t} - k \left(\frac{\partial^2 T}{\partial x^2} + \frac{\partial^2 T}{\partial y^2} \right) = Q \quad (3)$$

Where T is the temperature, t is time, ρ is the density, C_p is the specific heat capacity and k is the thermal

conductivity. Q is the net radiative and convective heat flux into the surface. The initial condition that governs the heat equation is:

$$T(x, y, t) = T_\infty \text{ at } t=0 \quad (4)$$

In Eqn.4, T_∞ , is the ambient temperature. An explicit forward-time, centred-space (FTCS) finite difference solution is used. The time derivative is replaced with a forward difference expression and the spatial derivative is replaced with a centred-difference expression as seen in Eqn.5. The FTCS scheme is conditionally stable and it was necessary to linearize the Stefan-Boltzmann equation through the radiative heat transfer coefficient, h_r .

$$(a) \frac{\partial T}{\partial t} = \frac{T_i^{n+1} - T_i^n}{\Delta t} \quad (5)$$

$$(b) \frac{\partial^2 T}{\partial x^2} = \frac{T_{i+1}^n - 2T_i^n + T_{i-1}^n}{\Delta x^2}$$

$$(c) \frac{\partial^2 T}{\partial y^2} = \frac{T_{i+1}^n - 2T_i^n + T_{i-1}^n}{\Delta y^2}$$

3 RESULTS AND DISCUSSION

Preparation of photocatalytic surfaces using NIR is two order of magnitude faster than production in a conventional convection oven as shown in the heat profiles in figure 2. The photoactivity is unaltered and there is no rutile transition that would limit this, despite high temperatures reached. This is likely to be due to short dwell time not allowing time for the kinetics of the change in crystal structure.

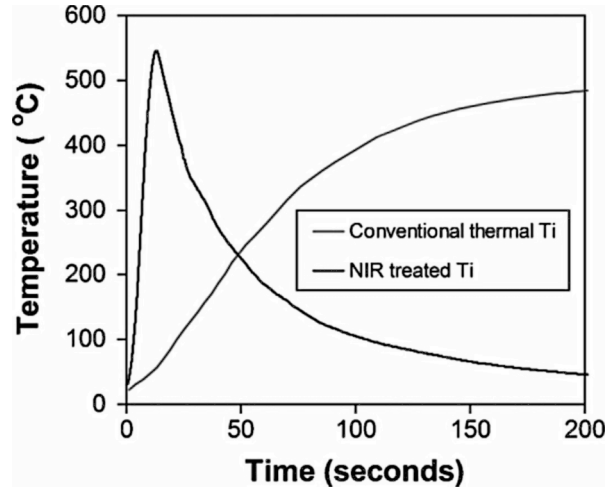


Figure 2: Typical heating profiles for NIR and convection cured samples shown for the first 200 s.

The time taken for absorbance of a 10ppm indigo carmine dye solution in deionised water to drop from an A value of 1 to 0.3 is consistently below 39.19 minutes using the TiO₂ based photocatalyst, down from >12 hours before refining of paste, deposition and sinter to incorporate nanoparticulate titania (figure 3). Now dwell times of 5 minutes have even been achieved with proprietary surface treatment.

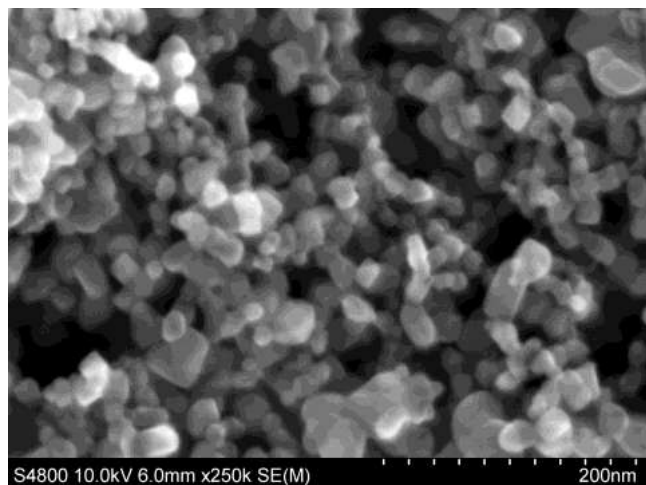


Figure 2: SEM image of porous TiO₂ layer

	ρ	α	T_s (K)	T_m (K)
TiO ₂ rich coating on metal substrate	0.69	0.31	339.75	345.10

Table 1: The total reflectance, ρ , total absorbance, α , and predicted, T_s , and measured, T_m , temperatures after an exposure of 4 seconds, with $T_c = 2600K$ and $\epsilon_{e=0.17}$

The computational model has been used to predict temperature profile achieved in a number of coating and substrate combinations and as can be seen in table 1, the application to TiO₂ shows a close correlation to the empirical data, suggesting a useful prediction here too.

4 CONCLUSIONS

TiO₂ based solutions for photocatalytic breakdown of dye effluents can help reduce environmental impact of textile industries. NIR enables rapid production, two orders of magnitude faster than conventional methods and the process can be computationally modelled. There are many other uses for these technologies and a number of further embodiments of the designs, beyond the scope of these proceedings. There is substantial ongoing work in NIR processing of various materials at lab and pilot scale, also significant work in water treatment and in building of computational models. These are all subjects of research papers currently being submitted to journals which give a fuller picture of the range of tests and possibilities for these systems. Water treatment initially focused on dyed effluent, but other avenues are being explored.

5 ACKNOWLEDGEMENTS

The authors would like to acknowledge financial support from the Engineering Physical Science Research Council (EPSRC EP/E035205) and colleagues at Tata Steel Europe and BASF coatings Ltd for their invaluable input. Des Brennan and Ashley Pursglove carried out research on the project whilst enrolled on the Steel Training Research and Innovation Partnership (STRIP). STRIP has been made possible by the EU's Convergence European Social Fund through the Welsh Government.

6 REFERENCES

- [1] Pursglove, EngD thesis, Swansea, 2015
- [2] Brogan and Monaghan, Composites: Part A 301-306, 1996.
- [3] Knischka, Lehmann, et al. Progress in Organic Coatings, 64, 171–174, 2009
- [4] Gowenlock, Mabbett and Worsley, JET, 2, 2, 2013
- [5] Watson, Mabbett, et al. Prog. Photovoltaics Res. Appl. 19, 482–486, 2011
- [6] Cherrington, Claypole, et al. J. Mater. Chem. 21, 562, 2011
- [7] Jewell, Mabbett and Searle, Lope-C, 2013
- [8] Bryant, Mabbett, et al. Organic Electronics: physics, materials, applications, 15, 6, 1126, 2014
- [9] Mabbett, Geary, et al. ECST, 50, 37, 155, 2012
- [10] Mabbett, Marinaccio, et al. ECST 2015
- [11] Charbonneau, Hooper, et al. Prog. Photovoltaics Res. Appl. 22, 12, 1267–1272, 2014
- [12] Mabbett, Elvins, et al. Prog. Org. Coat. 76, 1184–1190, 2013
- [13] Worsley and Searle, Mat Sci and Technology, 18, 6, 681-684, 2002
- [14] I. Mabbett, Elvins, et al. Prog. Org. Coat. 77, 494–501, 2014
- [15] O'Regan and Gratzel, Nature, 353, 737–740, 1991
- [16] Lee, Teuscher, et al. Science, 338, 6107, 643-647, 2012
- [17] Carnie, Charbonneau, et al. J. Mater. Chem. A. 1, 2225-2230, 2013
- [18] Troughton, Charbonneau, et al. J. Mater. Chem. A. 2015
- [19] Brennan, Mabbett, et al. Proceedings for ACME, Swansea, 2015
- [20] http://www.adphos.com/functionality_of_NIR_technology.html 02/04/2015
- [21] Lavery, Applied Mathematical Modelling, 2006.